Original Paper

Measurement and Analysis of Vibrations on the Trailer Bed, with Particular Attention to Velocity Kurtosis and Kurtosis Response Spectrum

Daichi NAKAI [*, **] and Katsuhiko SAITO [*]

The packaging vibration test in the laboratory is important to confirm the safety against vibration during distribution. Traditionally, the power spectral density is used as the test conditions. However, the real vibration during distribution is non-Gaussian, and many studies propose the vibration test methods considering its non-Gaussian. Non-Gaussian is conventionally represented by acceleration kurtosis or the probability density distribution of acceleration. According to current research, velocity kurtosis and kurtosis response spectrum are also crucial elements in vibration testing. However, there has been few research on the velocity kurtosis and there have been only a few researches on the kurtosis response spectrum of a real vibration. This study aims to measure the acceleration on the trailer bed and determine the non-Gaussian of the genuine vibration. Seven different routes, including highways and nonhighways, were used for driving tests. As the indicator of non-Gaussian, acceleration kurtosis, velocity kurtosis, kurtosis response spectra, and so on were calculated. Acceleration and velocity were both leptokurtic, with velocity kurtosis near to acceleration kurtosis. The values of kurtosis response varied with frequency. The contour of the kurtosis response spectrum became flattered as the damping factor was raised.

Keywords: Vibration Measurement, Acceleration Kurtosis, Velocity Kurtosis, Response spectrum, non-Gaussian Distribution

1. Introduction

The packaging vibration test in the laboratory is important to confirm the safety against vibration on the truck bed or the railways. It is necessary to assess the actual vibration measured on the truck bed to define the test conditions for the vibration test. The vibration levels in shipping have been studied in the United States [1, 2], China [3], Japan [4, 5], South-East Asia [2, 6-8], India [9, 10], Europe [11-13], and Brazil [14]. The feature quantities are calculated from the acceleration measured on the truck bed and are used as the vibration test condition. The Power Spectral Density (PSD) of acceleration is the most important vibration test condition. A random vibration test is often performed using only a PSD (traditional method). As a result, the PSD and root mean square (RMS) of acceleration, the integral of the PSD, have been reported in the majority of previous investigations.

It is pointed out that there are differences of acceleration kurtosis (K_a) and the probability density distribution of acceleration between the traditional method and the vibration measured on the truck bed [15, 16]. The probability density distribution of acceleration in a traditional method is Gaussian, and its acceleration kurtosis (K_a) is 3. Conversely, the probability density distribution of the real vibration has a larger skirt than the Gaussian distribution, and the real vibration is leptokurtic (K_a is greater than 3). The discrepancies are thought to be caused by the unevenness of the road surface as well as the vehicle's acceleration and deceleration. As a result, traditional methods may result in underpackaging. Several studies

* Transport Packaging Laboratory, Kobe University, 5-1-1, Fukaeminami, Higashinada, Kobe 658-0022, Japan
** Sankyu Inc. 46-51 Sakinohama, Nakabaru, Tobata, Kitakyushu, 804-0002, Japan
Corresponding author: Daichi Nakai. Tel: 093-883-8561 E-mail: d.nakai@sankyu.co.jp

have been carried out to improve the vibration test. In addition to PSD, these vibration generation studies take acceleration kurtosis, the probability density distribution of acceleration, or the RMS distribution into account [16-21].

Recently, the idea of the kurtosis response spectrum has been proposed [22]. The response is calculated using input acceleration using a Single-Degree of Freedom (SDOF) model and **Fig. 1** shows schematic of the kurtosis response spectrum. Since the previous studies used the absolute acceleration response and this study uses the acceleration applied inside the SDOF structure (proportional to the relative displacement response), **Fig. 1** is reconstructed from the cited paper. It is assumed that the higher the kurtosis response, the greater the risk of product damage, even if the PSD and the acceleration kurtosis are the same [23]. These studies show that the kurtosis response is not constant and changes depending on natural frequency values and damping factors [22, 23].

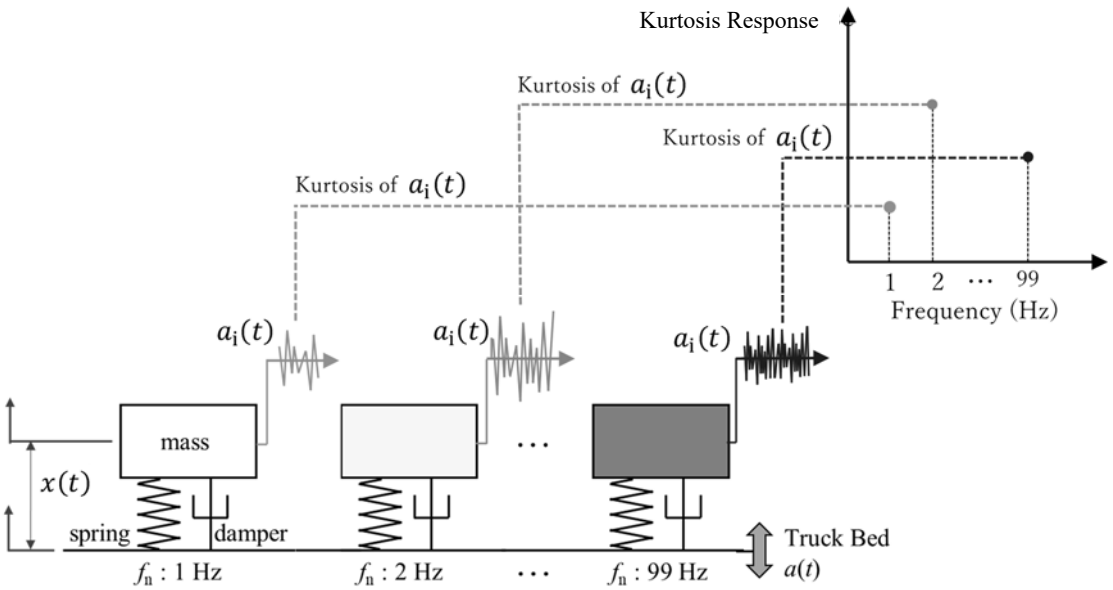

Fig. 1 Schematic of kurtosis response spectrum [based on Hosoyama et al.[22]].

Our previous study focused on velocity (integration of acceleration waveform), which is sometimes used as criteria of impact strength in shock fragility test or vibration strength in earthquake engineering [24, 25]. Moreover, the study proposed a method generating the time series acceleration with arbitrary acceleration kurtosis and velocity kurtosis (K_v) [26]. The closer the velocity kurtosis is to that of the real vibration, the closer to the kurtosis response spectrum is to that of the real vibration, even if the acceleration kurtosis is the same as that of the real vibration [27]. The vibration with the same K_a as that of the real vibration and K_v is smaller than that of the real vibration, the kurtosis response is significantly smaller than that of the real vibration at a low natural frequency range (20 Hz or less). However, no decrease in the kurtosis response spectrum was detected in the low natural frequency range in the vibration with the same K_a and K_v as the real vibration. In addition, our earlier research suggests a strategy for regulating the kurtosis response spectrum [27]. This method is characterized by the fact that the kurtosis is changed for each frequency component. Using this method makes it possible to generate vibrations with the same acceleration and velocity kurtosis but different response spectrum.

As described above, the studies about vibration test methods for packaging considering non-Gaussian nature have been advanced. However, there are not many studies of real transport measurements that report non-Gaussian nature. For example, only some studies reported K_a which is the most major statistic for non-Gaussian nature [3, 13, 19]. Furthermore, the previous studies about kurtosis response spectra measured on the roads were by a small van only [22, 23, 28]. Moreover, no studies that we are aware of have examined several real vibrations about the K_v. As a result, the non-Gaussian nature of genuine vibration remains unknown.

The aims of this study are as follows:

- To clarify K_v and the probability density distribution of velocity.
- To clarify the kurtosis response spectrum on the trailer bed.
- To report K_a and the probability density distribution of acceleration on the trailer bed.

2. Experiment

2.1 Test vehicle

Fig. 2 shows the trailer (maximum load: 13.2 ton, Air Suspension) used in this study. The surface of the trailer bed was made of wood. Dummy weights (5.6 tonf) were eight steel members, each with a size of 7000×300×300 mm. The dummy weights were placed in front of the trailer and were placed in two stacks. **Fig. 3** shows the positions of the dummy weights on the truck bed.

Fig. 2 The photo of the trailer and dummy weight.

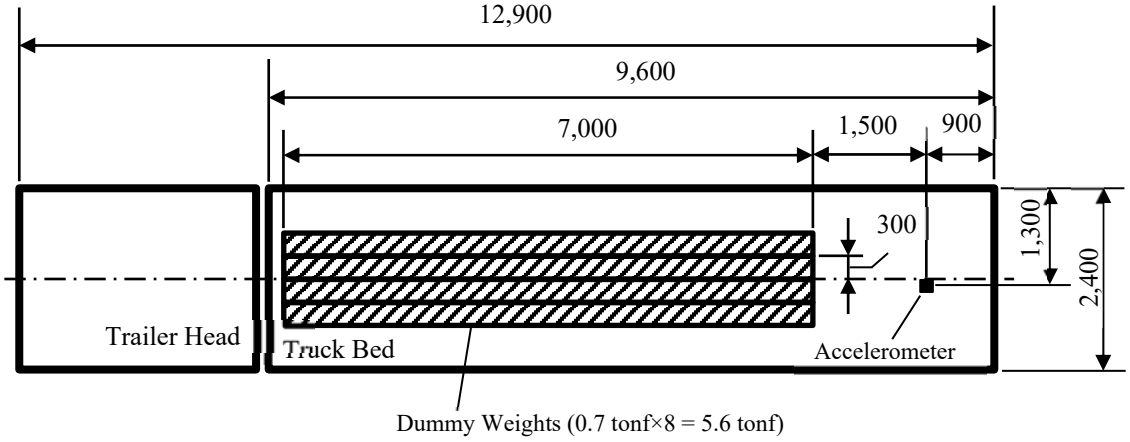

Fig. 3 Positions of dummy weights and the accelerometer on the truck bed.

2.2 Accelerometer

The accelerometer was DER-1000 (SHINYEI Technology Co., LTD.). The bottom of the DER-1000 was attached to the trailer bed with double-sided tape and was fixed with adhesive tape to prevent the accelerometer from moving. The accelerometer data logger was attached in the rear center of the trailer. **Fig. 3** shows a schematic of the position where the accelerometer was attached.

The accelerometer was recorded on three axes: lateral, longitudinal, and vertical. The sampling frequency of the accelerometer was 1,000 Hz. The greatest acceleration was 490 m/s^2. There was no impact or time trigger set, and all acceleration data were recorded throughout driving testing, including when the car was paused due to traffic signals or the like. After the test was completed, high-frequency components were removed from the acceleration waveform using a 100 Hz low-pass filter [27].

2.3 Test route

Table 1 shows the test routes and conditions. Experiments were conducted in Tokyo (the largest city in Japan) and its suburbs. In this study, we ran both highway and nonhighway and analyzed them separately. Route (a) and (b) are the outbound route, and routes (c) and (d) are the inbound route. Therefore, routes (c) and (d) are, respectively, in the opposite lane of the route (a) and (b). Times in Table 1 show the analyzed time preprocessed by the method described in Chapter 3.2 with the stopping section removed. Average speeds in Table 1 were calculated from the Distances and Times in **Table 1**. The detailed test routes are shown in **Fig. 4** and **5**. The lines added on the map show the routes the trailer ran during driving tests.

Table 1 Test routes and conditions.

Route	Departure point	Arrival point	Road	Dummy Weight (tonf)	Distance (km)	Time (s)	Average Speed (km/h)
(a)	Higashi-Ogishima Interchange	Chiba-kita Interchange	Highway	0	57	2,856	72
(b)	Chiba-kita Interchange	Yachiyo city	Nonhighway	0	17	1,129	54
(c)	Yachiyo city	Chiba-kita Interchange	Nonhighway	5.6	17	1,176	52
(d)	Chiba-kita Interchange	Higashi-Ogishima Interchange	Highway	5.6	57	3,034	68
(e)	Rinkai-fukutoshin Interchange	Tokyo Interchange	Highway	5.6	21	861	88
(f)	Tokyo Interchange	Nakai Parking Area	Highway	5.6	53	2,950	65
(g)	Gotenba city	Kawasaki city	Nonhighway	5.6	101	10,040	36

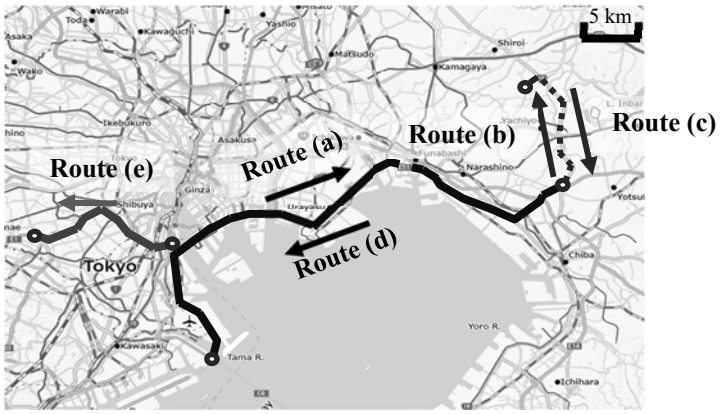

Fig. 4 The test route from (a) to (e) [29].

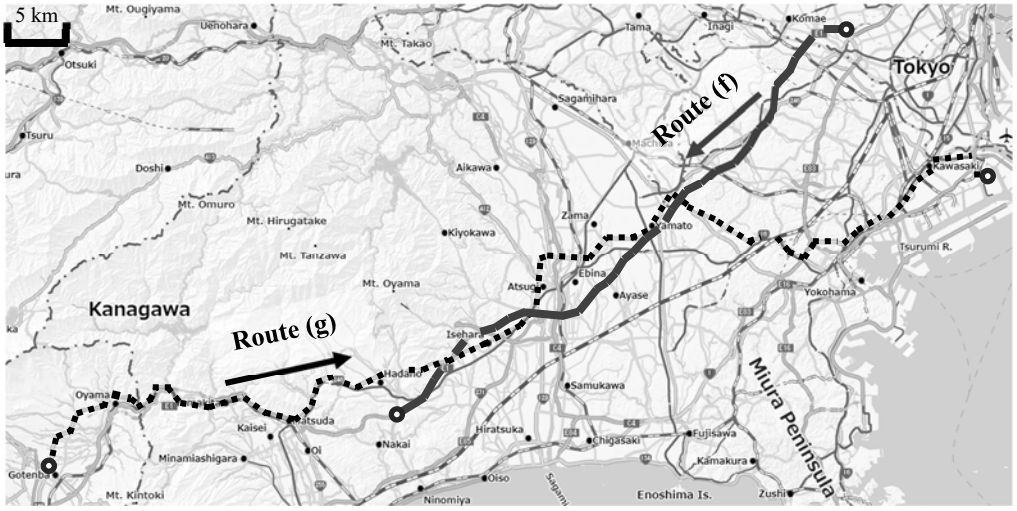

Fig. 5 The test route from (f) to (g) [29].

3. Calculation

3.1 Estimation of velocity

The Fourier transform of velocity $V(f)$ was calculated by equation (1):

$$V(f) = \frac{L(f)A(f)}{2\pi i f}, \quad (1)$$

where, $L(f)$, and $A(f)$ are respectively the low-cut filer, and the Fourier transform of acceleration [30]. $L(f)$ is a third-order Butterworth filter, and the cutoff frequency is 0.5 Hz. The time series velocity $v(t)$ was calculated from $V(f)$ using an inverse Fourier transform.

3.2 Moving RMS and the estimation of the stopping section

In the case of nonhighway, there are stop sections such as traffic lights even when the trailer is on the road. While the time when the trailer is halted is included, the RMS value of the entire vibration is reduced, and the vibration during transportation may be underestimated. As a result, it is vital to distinguish between the time the trailer is running and the paused sections.

In this study, the moving RMS (vertical direction) was used to determine the stopping section. First, we divided the vibration in the vertical axis direction into 0.5 second intervals. The RMS value was then determined for each 0.5 second. Segments with low RMS values in the vertical axis direction were considered halted and were eliminated from the study in all directions: lateral, longitudinal, and vertical. As a stop segment, a value of 0.08 m/s^2 was set. This is due to the probability density distribution of moving RMS having a local minimum value of about 0.08 m/s^2, as explained in Chapter 4.

3.3 Response spectrum

The same way calculated the response spectrum as in our previous study [26, 27]. A SDOF system as shown in **Fig. 1** is expressed by equation (2):

$$m\left(\frac{d^2x(t)}{dt^2} + a(t)\right) + c\frac{dx(t)}{dt} + kx(t) = 0, \quad (2)$$

where $t, m, c, k, a(t)$ and $x(t)$ respectively, time, the mass, viscosity coefficient, spring constant, the time series acceleration on the truck bed, and the relative displacement between the mass and the trailer bed. An impulse response function of the relative displacement $f(t)$ is expressed by equation (3):

$$f(t) = \frac{1}{\omega_d} e^{-h\omega_n t} sin\omega_d t, \quad (3)$$

where ω_n, ω_d, and h are, respectively, undamped natural angular frequency, and damped natural angular frequency of the response and the damping factor. In this system, a natural angular frequency ω_n equals to $\sqrt{k/m}$ and a natural frequency f_n is $\omega_n/2\pi$. The damping factor, h is expressed by equation (4):

$$h = \frac{c}{2m\omega_n}. \quad (4)$$

The damped natural angular frequency, ω_d is expressed by equation (5):

$$\omega_d = \omega_n\sqrt{1-h^2}. \quad (5)$$

$x(t)$ is expressed by the equation (6):

$$x(t) = \int_o^t a(\tau) f(t-\tau) d\tau, \quad (6)$$

where τ is a parameter. Equation (6) is a convolution integral; therefore, $x(t)$ can be calculated by equation (7):

$$x(t) = \frac{1}{2\pi}\int_{-\infty}^{\infty} A(f)F(f)e^{2i\pi ft}\, df, \quad (7)$$

where $A(f)$ and $F(f)$ are the Fourier transform of $a(t)$ and $f(t)$, respectively. The acceleration applied inside the SDOF structure $a_i(t)$ is proportional to the relative displacement $x(t)$:

$$a_i(t) = \frac{k}{m}x(t) = 4\pi^2 f_n^2 x(t). \quad (8)$$

Here, f_n is from 1 to 100 Hz at intervals of 0.5 Hz. The RMS and kurtosis of $a_i(t)$ calculated for each natural frequency f_n by fixing the damping factor with h, are the RMS response spectrum $R_h(f)$ and the kurtosis response spectrum $K_h(f)$.

4. Results and Discussion

Fig. 6 shows the probability density distribution of moving RMS on the vertical axis. The dotted line represents the threshold of moving RMS. **Fig. 6** (a), (d), (e), and (f) were the results when the trailer ran on the highway. There are no traffic signals because of driving on highways, and few sections with RMS values below 0.08 m/s^2 are considered stop sections. Moreover, **Fig. 6** (b), (c), and (g) are the results when the trailer ran on nonhighway. The local minimum of the probability density distribution of the moving RMS was recorded around 0.08 m/s^2 for all the nonhighway routes. Therefore, it is statistically valid to set the threshold value at 0.08 m/s^2 in this study.

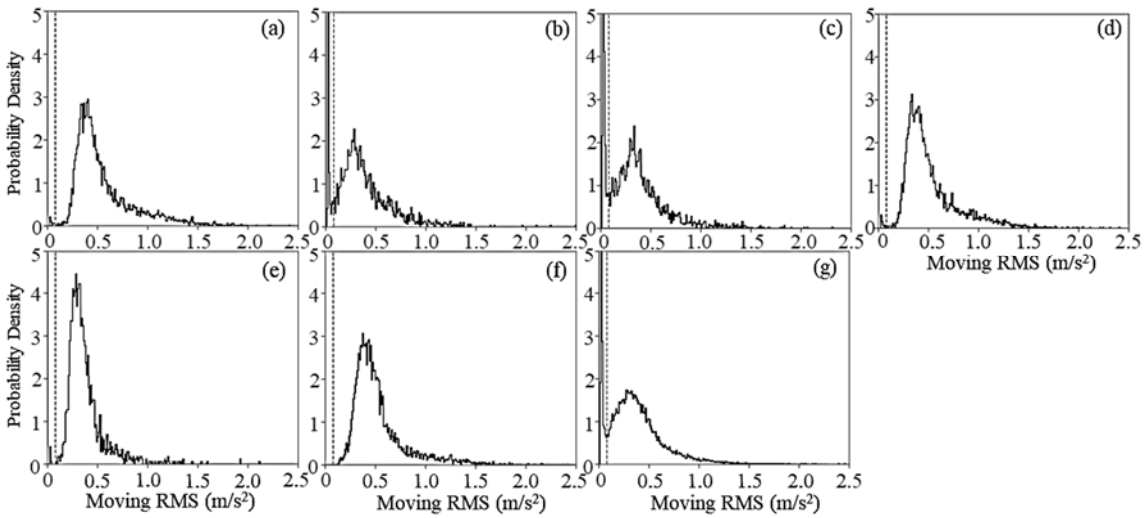

Fig. 6 The probability density distribution of moving RMS (Vertical Axis).

Table 2 displays the acceleration and velocity statistics that were preprocessed using the method outlined in Chapter 3.2. The RMS levels of acceleration and velocity in the longitudinal direction were the lowest of all directions. The lateral direction has the highest acceleration RMS levels of all directions. The vertical direction has the greatest velocity RMS levels of all directions. Both skewnesses of acceleration and velocity were close to 0, and no clear asymmetry was observed. K_a and K_v were leptokurtic and much larger than 3 for all values. For example, Zhou et al. have reported the K_a between 3.94-24.3 [3]. Therefore, the results of the K_a in this study are within the range reported in the previous studies. On the other hand, since there are few previous studies about K_v, it is difficult to compare with previous studies. But it is reasonable that K_v are also leptokurtic because K_a are leptokurtic.

Routes (a) and (d) are outward and inward on the same route, although there is a difference in the presence of the dummy weights or not. Since there was no clear difference between these two tests, it is assumed that the vibration levels in this test mainly depended on the road surface condition and driving speed rather than the presence of the dummy weights.

The difference between highway and nonhighway was not clear in terms of RMS levels, as the smallest RMS level for vertical acceleration was Route (e) [highway], and the largest RMS level for vertical acceleration was route (a) [highway]. K_a in the vertical direction for nonhighway [Routes (b), (c) and (g)] was larger than that for highway [Routes (a), (d), (e) and (f)]. Further, there was no clear difference between K_v in the vertical direction of the nonhighway and that of the highway. There were different trends between the acceleration and velocity statistics because the vibration in the low-frequency region has a larger effect on the velocity than the acceleration.

Table 2 Statistical Values of Vibrations

	Stats	Direction	Route (a)	Route (b)	Route (c)	Route (d)	Route (e)	Route (f)	Route (g)
Acceleration	RMS (m/s^2)	Lateral	0.99	0.74	0.62	0.91	0.52	0.89	0.50
		Longitudinal	0.18	0.15	0.16	0.19	0.14	0.19	0.15
		Vertical	0.63	0.49	0.51	0.60	0.42	0.60	0.51
	Skewness	Lateral	−0.01	0.06	−0.10	−0.07	0.01	0.09	0.01
		Longitudinal	0.04	−0.01	0.02	0.07	0.00	−0.03	−0.03
		Vertical	−0.02	0.11	0.12	0.02	−0.01	0.03	0.05
	Kurtosis	Lateral	12.99	12.35	13.36	12.93	8.75	16.99	14.53
		Longitudinal	9.20	9.81	8.44	9.86	6.64	7.59	14.69
		Vertical	8.77	10.97	12.38	8.89	10.25	10.05	12.14
Velocity	RMS (m/s)	Lateral	0.0127	0.0102	0.0083	0.0110	0.0063	0.0106	0.0065
		Longitudinal	0.0016	0.0013	0.0013	0.0015	0.0010	0.0013	0.0011
		Vertical	0.0180	0.0114	0.0111	0.0150	0.0095	0.0145	0.0109
	Skewness	Lateral	0.08	0.03	0.16	0.03	−0.01	0.13	−0.04
		Longitudinal	0.13	0.00	−0.01	0.07	−0.17	−0.03	−0.01
		Vertical	0.08	0.03	0.16	0.03	−0.01	0.13	−0.04
	Kurtosis	Lateral	11.05	11.34	12.87	11.08	8.65	15.01	10.47
		Longitudinal	11.04	6.25	8.30	7.69	8.47	8.73	12.83
		Vertical	9.18	8.42	9.03	8.65	10.28	9.13	10.02

Fig. 7 shows the PSDs of acceleration. In the lateral axis, there was a peak around 15 Hz. In the longitudinal axis, there was almost no vibration component below 10 Hz. In the vertical axis, there were peaks at 5 Hz and 12 Hz. 12 Hz was assumed to be the peak caused by the vibration of the tires [31]. In general, the natural frequency caused by suspension and tire vibration decreases with cargo loading. However, no discernible difference was seen in this investigation between the routes (a) and (b) without the dummy weight and the routes (d) and (c) with the dummy weight.

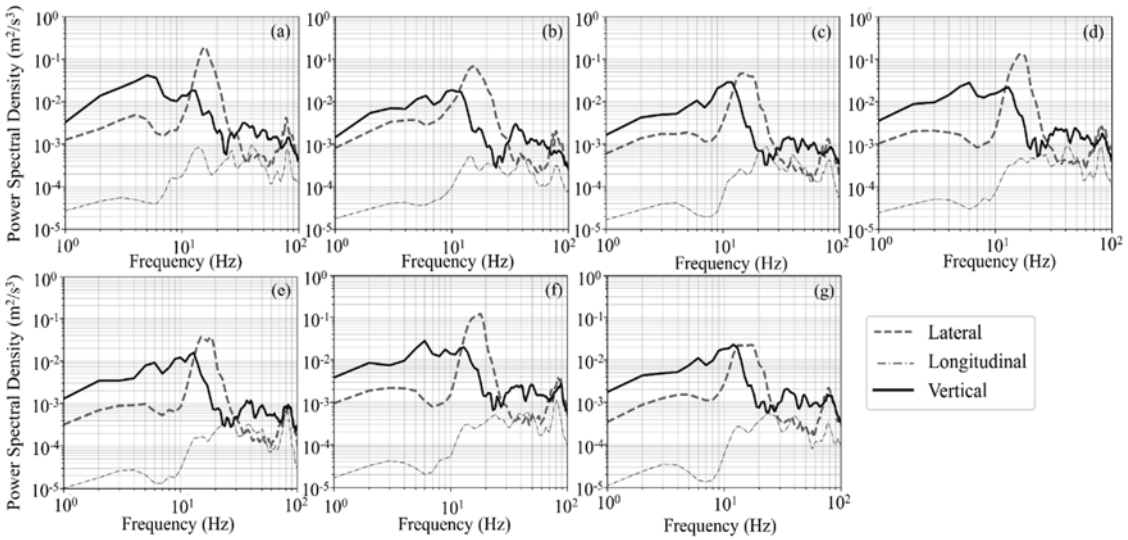

Fig. 7 The power spectral densities of acceleration.

The probability density distributions of acceleration are depicted in **Fig. 8**. The probability density distribution of acceleration in the lateral direction is substantially wider than that in the vertical direction in routes (b), (d), and (f). However, in the routes (e) and (g), there was no discernible variation between the probability density distributions in the vertical and lateral directions.

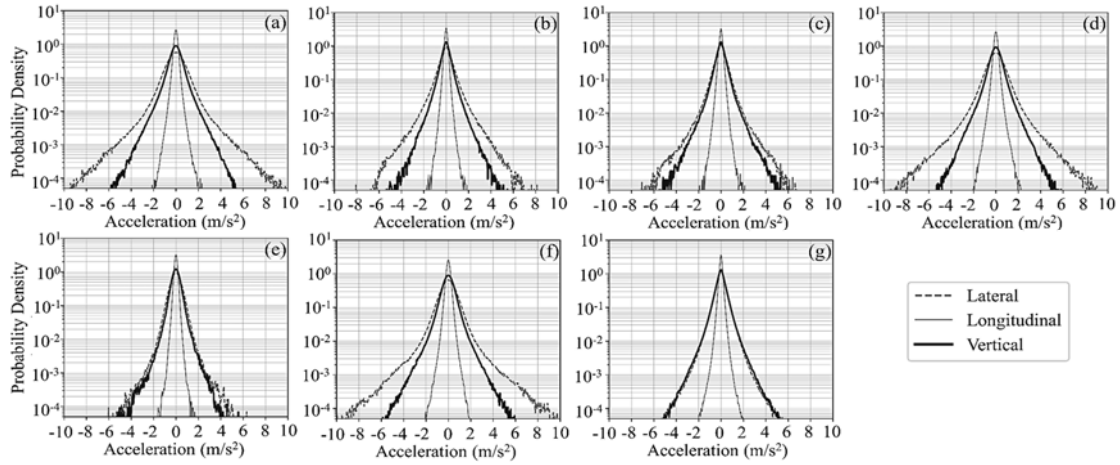

Fig. 8 The probability density distributions of acceleration.

Fig. 9 shows the probability density distributions of velocity. The spread of the probability density distribution was narrower for the longitudinal axis than for the other orientations. Unlike the probability density distribution of acceleration, the vertical axis had the greatest spread in the probability density distribution of velocity.

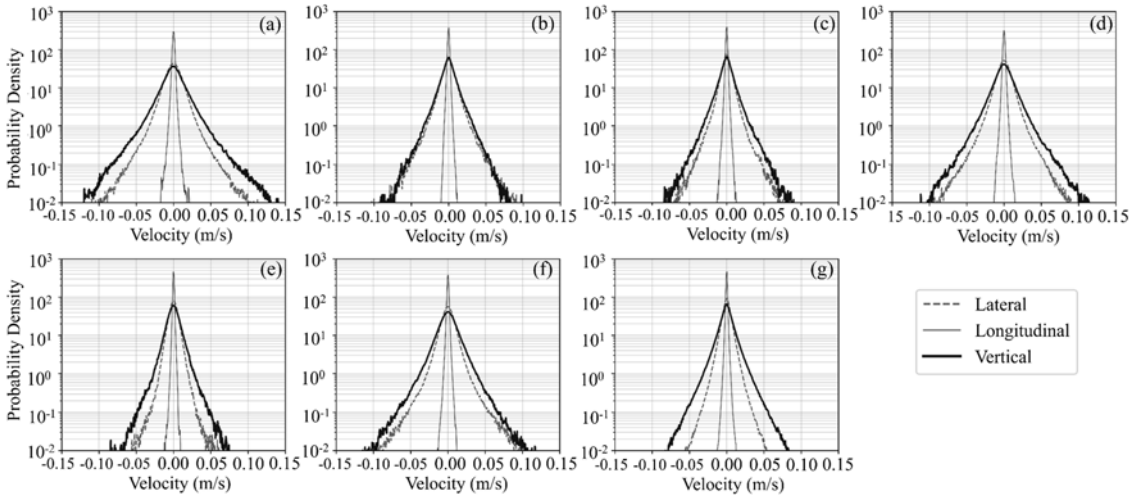

Fig. 9 The probability density distributions of velocity.

Fig. 10 shows the $R_h(f)$ of vertical direction. The local maximum of the $R_h(f)$ for most of the routes was around 12 Hz. As h increased, the $R_h(f)$ values decreased, and the effect of natural frequency on the $R_h(f)$ became smaller.

Fig. 11 shows the $K_h(f)$ of the vertical direction. All $K_h(f)$ values are above 3, and the response vibrations were leptokurtic. Previous studies which used the small van have also reported that the absolute acceleration response is leptokurtic [22, 28]. Therefore, the results of $K_h(f)$ in this study are also assumed to be valid. The local maximum of $K_h(f)$ around 12 Hz became smaller as h became larger. In the case of the natural frequency values where $K_h(f)$ was smaller than the surrounding frequencies, $K_h(f)$ became larger as h became larger. As a result, the effect of the natural frequency on $K_h(f)$ became smaller as h increased. Previous study which used the small van has also reported the same effect of natural frequency and h [22].

Comparing **Fig. 10** and **Fig. 11**, some of the natural frequencies of the peak of $R_h(f)$ and the peak of the natural frequency of $K_h(f)$ coincided with each other. The most obvious oscillation is the tire-induced peak around 11-13 Hz; the local maximum values around 11-13 Hz of $K_h(f)$ for the nonhighway [Routes (c) and (g)] are 13.0 and 12.5 Hz, respectively. In the case of highway [Routes (d), (e) and (f)], the peaks around 11-13 Hz of $R_h(f)$ and $K_h(f)$ are 11.5, 12.5, and 13.0 Hz, respectively. There were also cases where $K_h(f)$ was a local minimum at the natural frequency where $K_h(f)$ was a peak. For example, in route (f), $K_h(f)$ reached a peak around 87.0 Hz (**Fig. 10**), and $K_h(f)$ reached a local minimum value around 88.0 Hz (**Fig. 11**).

On the other hand, some of the natural frequencies of the peak of $R_h(f)$ and the peak of the natural frequency of $K_h(f)$ did not coincided with each other. For example, in the case of routes (a) and (b), the RMS response spectra have the peaks around 12.0 Hz as shown in **Fig. 10**(a) and (b), but there were no local maxima or minima around 12.0 Hz for the kurtosis response spectrum as shown in **Fig. 11**(a) and (b). Although routes (a) and (b) were without dummy weights, it is not possible to determine whether dummy weights have the effect on $K_h(f)$ because of the insufficient number of the experiments in this study.

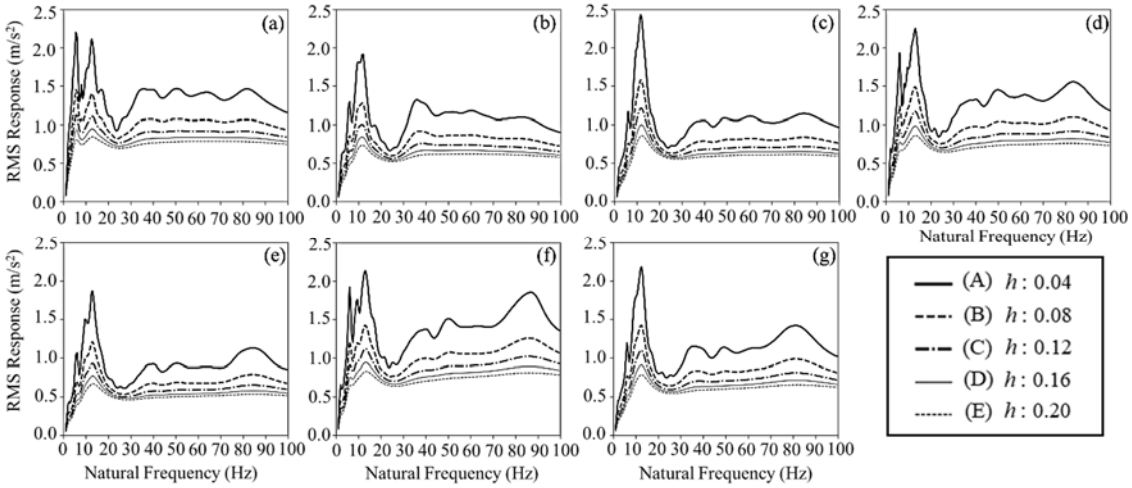

Fig. 10 The RMS response spectra (vertical axis),
(A) $h = 0.04$, (B) $h = 0.08$, (C) $h = 0.12$, (D) $h = 0.16$, (E) $h = 0.20$.

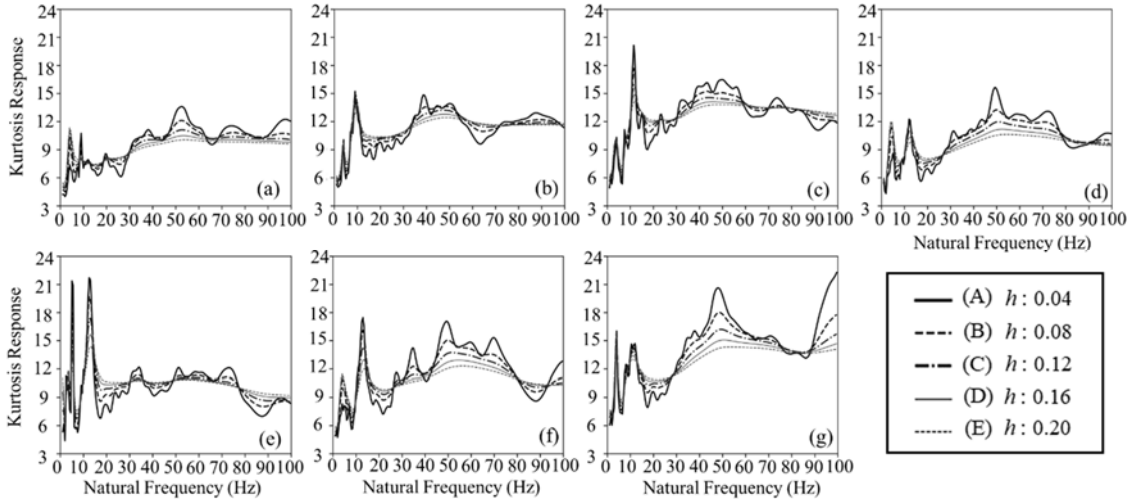

Fig. 11 The Kurtosis response spectra (vertical axis),
(A) $h = 0.04$, (B) $h = 0.08$, (C) $h = 0.12$, (D) $h = 0.16$, (E) $h = 0.20$.

5. Conclusions

In this study, the vibrations were measured on the trailer bed and analyzed. The study concludes the following:

- Acceleration and velocity were both leptokurtic. The velocity kurtosis was nearly identical to the acceleration kurtosis.
- The probability density distribution of acceleration tended to be widest in the lateral direction. On the other hand, the probability density distribution of velocity tended to be widest in the vertical direction. This is because the vibration in the low-frequency region has a larger effect on the velocity than the acceleration.
- The values of kurtosis response were leptokurtic and varied with frequency. This result agrees with the previous studies by the small van.

- As the damping factor increased, the shape of the kurtosis response spectrum became flatter. This result agrees with the previous study by the small van.
- Some frequencies at which the local maximum or minimum values of the kurtosis response spectrum coincided with the frequencies at which the maximum local values of the RMS response spectrum were.

References

1) J. Singh, S. P. Singh and E. Joneson, Measurement and analysis of US truck vibration for leaf-spring and air-ride suspensions, and development of tests to simulate these conditions, Packag. Technol. Sci., **19**(6), p309 (2006).
2) V. Chonhenchob, S. P. Singh, J.J. Singh, J. Stallings and G. Grewal, Measurement and analysis of vehicle vibration for delivering packages in small-sized and medium-sized trucks and automobiles, Packag. Technol. Sci., **25**(1), p31 (2012).
3) H. Zhou and Z. W. Wang, Measurement and analysis of vibration levels for express logistics transportation in South China, Packag. Technol. Sci., **31**(10), p665 (2018).
4) F. Lu, Y. Ishikawa, T. Shiina and T. Satake, Analysis of shock and vibration in truck transport in Japan, Packag. Technol. Sci., **21**(8), p479 (2008).
5) F. Lu, Y. Ishikawa, H. Kitazawa and T. Satake, Effect of vehicle speed on shock and vibration levels in truck transport, Packag. Technol. Sci., **23**(2), p101 (2010).
6) B. Jarimopas, S. P. Singh and W. Saengnil, Measurement and analysis of truck transport vibration levels and damage to packaged tangerines during transit, Packag. Technol. Sci., **18**(4), p179 (2005).
7) V. Chonhenchob, S. P. Singh, J. J. Singh, S. Sittipod, D. Swasdee and S. Pratheepthinthon, Measurement and analysis of truck and rail vibration level in Thailand, Packag. Technol. Sci., **23**(2), p91 (2010).
8) M. P. Kurniawan, V. Chonhenchob, S. P. Singh and S. Sittipod, Measurement and analysis of vibration levels in two and three wheel delivery vehicles in Southeast Asia, Packag. Technol. Sci., **28**(9), p836 (2015).
9) S. P. Singh, A. P. S. Sandhu, J. Singh and E. Joneson, Measurement and analysis of truck and rail shipping environment in India, Packag. Technol. Sci., **20**(6), p381 (2007).
10) S. P. Singh, K. Saha, J. Singh and A. P. S. Sandhu, Measurement and analysis of vibration and temperature levels in global intermodal container shipments on truck, rail and ship, Packag. Technol. Sci., **25**(3), p149 (2012).
11) M. A. Garcia-Romeu-Martinez, S. P. Singh and V. A. Cloquell-Ballester, Measurement and analysis of vibration levels for truck transport in Spain as a function of payload, suspension and speed, Packag. Technol. Sci., **21**(8), p439 (2008).
12) P. Böröcz and S. P. Singh, Measurement and analysis of vibration levels in rail transport in Central Europe, Packag. Technol. Sci., **30**(8), p361 (2017).
13) P. Böröcz and S. P. Singh. Measurement and analysis of delivery van vibration levels to simulate package testing for parcel delivery in Hungary, Packag. Technol. Sci., **31**(5), p342 (2018).
14) G. O. Rissi, S. P. Singh, G. Burgess and J. Singh, Measurement and analysis of truck transport environment in brazil, Packag. Technol. Sci., **21**(4), p231 (2008).
15) J. Lepine, V. Rouillard, M. A. Sek, Review paper on road vehicle vibration simulation for packaging testing purposes, Packag. Technol. Sci., **28**(8), p672 (2015).
16) V. Rouillard, M. A. Sek, Synthesizing non-stationary, non-Gaussian random vibrations, Packag. Technol. Sci., **23**(8), p423 (2010).

17) S. R. Winerstein, Nonlinear vibration models for extremes and fatigue, Eng. Mech., 114(10), p1772 (1988).
18) A. Hosoyama, and T. Nakajima, The Method of Generating Non-gaussian Random Vibration Using Kurtosis, J. Packag. Sci. Technol. Jpn., **20**(1), p27 (2011).
19) V. Rouillard, On the non-Gaussian Nature of Random Vehicle Vibrations, Proceedings of The World Congress on Engineering, p1219 (2007).
20) K. R. Griffiths, B. J. Hicks, P. S. Keogh and D. Shires, Wavelet analysis to decompose a vibration simulation signal to improve pre-distribution testing of packaging. Mech. Syst. Signal Process, **76-77**, p780 (2015).
21) H. Zhou and Z. W. Wang, A new approach for road-vehicle vibration simulation, Packag. Technol. Sci., **31**(5), p246 (2018).
22) A. Hosoyama, K. Tsuda and S. Horiguchi, Development and validation of kurtosis response spectrum analysis for antivibration packaging design taking into consideration kurtosis, Packag. Technol. Sci., **33**(2), p51 (2020).
23) A. Hosoyama, K. Tsuda and S. Horiguchi, Non-Gaussian nature of the SDOF response to Gaussian vehicle vibrations, J. Packag. Sci. Technol. Jpn, **30**(4), p243 (2021).
24) R. E. Newton, Fragility Assessment Theory and Test Procedure, Monterey, CA: Monterey Research Laboratory, Inc (1968).
25) A. Masuda, K. Nagato and H. Kawase, Study on construction of vulnerability by earthquake response analysis for reinforced concrete buildings, J. Struct. Constr. Eng., AIJ, **558**, p101(2002).
26) D. Nakai and K. Saito, A method for generating random vibration using acceleration kurtosis and velocity kurtosis, J. Appl. Packag. Res., **11**(2), p64 (2019).
27) D. Nakai and K. Saito, A method for generating random vibration considering kurtosis response spectrum, J. Packag. Sci. Technol. Jpn., **30**(4), p261 (2021).
28) A. Hosoyama, K. Tsuda and S. Horiguchi, Ippandō sōkōzi ni keisoku sareta nidai shindō no sendo ōtō supekutoru kaiseki (In Japanese), Proceedings of 29th annual meeting of the Society of Packaging Science & Technology, Japan, p82 (2020).
29) Geospatial Information Authority of Japan, https://maps.gsi.go.jp/multil/index.html, (August 30, 2021).
30) D. Nakai and K. Saito, Estimation method of velocity change on truck bed, J. Packag. Sci. Technol. Jpn., **28**(1), p33 (2020).
31) V. Rouillard, Generating road vibration test schedules from pavement profiles for packaging optimization, Packag. Technol. Sci., **21**(8), p501 (2008).

（Received　13January 2022）
（Accepted　10June 2022）

速度の尖度と尖度応答スペクトルに注目した トレーラー荷台振動の測定と分析

中 井　太 地 [*,**]，　斎 藤　勝 彦 [*]

包装貨物振動試験は、流通時の振動に対する安全性を確認するために実施される。一般的に試験条件としてパワースペクトル密度が使用されている。それに加えて非ガウス性を考慮した振動試験方法が研究されおり、非ガウス性は加速度の尖度で評価されている。近年、速度の尖度と尖度応答スペクトルも振動試験の重要な要素であることが示されているが、これらの指標の実振動計測事例はほとんど存在しない。実振動の加速度を測定し、非ガウス性を評価することが本研究の目的である。輸送試験は、高速道路と一般道を含む 7 つのルートで行った。非ガウス性の指標として、加速度の尖度、速度の尖度、尖度応答スペクトルなどで評価した。加速度と速度の尖度は、ガウス分布の値である 3 より大きく、両方の値は近かった。尖度応答の値は周波数に応じて変化し、減衰係数が大きくなるに従い、尖度応答スペクトルの形状は平坦になった。

キーワード:　振動測定, 加速度の尖度, 速度の尖度, 応答スペクトル, 非ガウス分布